Near-bed stratification controls bottom hypoxia in ice-covered alpine lakes

Journal Article

Author(s):
Perga, Marie-Elodie; Minaudo, Camille; Doda, Tomy; Arthaud, Florent; Beria, Harsh ⓘD; Chmiel, Hannah E.; Escoffier, Nicolas; Lambert, Thibault; Napolleoni, Raphaelle; Obrador, Biel; Perolo, Pascal; Rüegg, Janine; Ulloa, Hugo; Bouffard, Damien

Near-bed stratification controls bottom hypoxia in ice-covered alpine lakes

Marie-Elodie Perga [1,2]* Camille Minaudo [3,4] Tomy Doda [5] Florent Arthaud,[6] Harsh Beria,[7] Hannah E. Chmiel,[4] Nicolas Escoffier [1] Thibault Lambert,[1] Raphaelle Napolleoni,[8] Biel Obrador [9] Pascal Perolo [1] Janine Rüegg,[1] Hugo Ulloa [10] Damien Bouffard [1,5]

[1]Faculty of Geoscience and Environment, University of Lausanne, Lausanne, Switzerland
[2]Geopolis, UNIL (on behalf of the Lacs Sentinelles Network), Lausanne, Switzerland
[3]Department of Evolutionary Biology, Ecology and Environmental Sciences, University of Barcelona, Barcelona, Spain
[4]Physics of Aquatic Systems Laboratory, Margaretha Kamprad Chair, Institute of Environmental Engineering, École Polytechnique Fédérale de Lausanne, Lausanne, Switzerland
[5]Department of Surface Waters—Research and Management, Eawag, Swiss Federal Institute of Aquatic Science and Technology, Kastanienbaum, Switzerland
[6]UMR CARRTEL, University Savoie-MontBlanc, Le Bourget du Lac, France
[7]Department of Environmental Systems Science, ETH Zurich, Zurich, Switzerland
[8]ASTERS (on behalf of the Lacs Sentinelles Network), Pringy, France
[9]Institut de Recerca de la Biodiversitat (IRBio), University of Barcelona, Barcelona, Spain
[10]Department of Earth and Environmental Science, University of Pennsylvania, Philadelphia, Pennsylvania

Abstract

In ice-covered lakes, near-bottom oxygen concentration decreases for most of the wintertime, sometimes down to the point that bottom waters become hypoxic. Studies insofar have reached divergent conclusions on whether climate change limits or reinforces the extent and duration of hypoxia under ice, raising the need for a comprehensive understanding of the drivers of the dissolved oxygen (DO) dynamics under lake ice. Using high-temporal resolution time series of DO concentration and temperature across 14 mountain lakes, we showed that the duration of bottom hypoxia under ice varies from 0 to 236 d within lakes and among years. The variability of hypoxia duration was primarily explained by changes in the decay rate of DO above the lake bottom rather than by differences in DO concentration at the ice onset or in the ice-cover duration. We observed that the DO decay rate was primarily linked to physical controls (i.e., deep-water warming) rather than biogeochemical drivers (i.e., proxies for lake or catchment productivity). Using a simple numerical model, we provided a proof-of-concept that the near-bed stratification can be the mechanism tying the DO decay rate to the sediment heat release under the ice. We ultimately showed that the DO decay rate and hypoxia duration are driven by the summer light climate, with faster oxygen decline found under the ice of clearer cryostratified alpine lakes. We derived a framework theorizing how the hypoxia duration might change under the ice of alpine lakes in a warmer climate.

*Correspondence: marie-elodie.perga@unil.ch

Additional Supporting Information may be found in the online version of this article.

The cryosphere is shrinking at well-documented rates, but the far-reaching ecosystemic implications of ice loss remain poorly anticipated (Fountain et al. 2012). This holds for cryosphere features such as sea ice, snow, and glaciers, with lake ice making no exception. Current changes in the phenology and extent of lake ice have been regularly updated and refined since the seminal work by Magnuson et al. (2000). A recent field-based study estimated that the ice cover of Northern hemisphere lakes has, on average, shortened by 17 d over the last century (Sharma et al. 2021). Significant achievements in remote sensing allow the monitoring of lake ice phenology where ground data are scarce (Wang et al. 2021). Deterministic or data-driven modeling approaches can predict the vulnerability of currently dimictic lakes to permanent ice loss until the end of

the century (Woolway and Merchant 2019; Caldwell et al. 2021) as well as more continuous changes in ice phenology (Råman Vinnå et al. 2021). While the modifications of winter ice conditions and phenology are expected to result in major rearrangements of physical and ecological processes in lakes losing ice cover, most still have to be evidenced and quantified (Salonen et al. 2009; Hampton et al. 2017; Cavaliere et al. 2021).

Pioneering investigations of the processes occurring under lake ice had to build on a limited number of observations due to the difficulty of sampling (Mortimer and Mackereth 1958). The development of sensor technology combined with a renewed interest in wintertime limnology has generated large amounts of high-resolution data over the last decade. However, rather than clearing up the picture, recent studies have unveiled diverse and complex physical, biogeochemical, and ecological processes occurring under the ice (Obertegger et al. 2017; Song et al. 2019; Zdorovennova et al. 2021). Conceptual frameworks have been developed to unify pioneering and more recent knowledge of under-ice processes and derive assumptions on the ecological consequences of a changing ice cover on lakes (Cavaliere et al. 2021; Jansen et al. 2021). All conceptual frameworks place dissolved oxygen (DO) concentrations under the ice as a central variable both integrating the ecological responses to changing wintertime conditions and determining the effects of ice phenology alteration on the following seasons (Cavaliere et al. 2021; Jansen et al. 2021).

Processes acting upon DO under the ice can include a significant amount of primary production, depending on the thickness and optical properties of the ice (Zdorovennova et al. 2021). The DO stock under the ice nevertheless diminishes with time due to the lake surface isolation from the atmosphere and the predominance of heterotrophy (Leppi et al. 2016; Obertegger et al. 2017; Song et al. 2019). Therefore, in many ice-covered lakes, the near-bottom oxygen concentration decreases for most of the wintertime, sometimes down to the point that bottom waters become hypoxic (Mathias and Barica 1980; Malm et al. 1998; Stefanovic and Stefan 2002). The vertical extent of the hypoxic layer and duration of hypoxia determine the availability of oxic refuges for many organisms actively overwintering under the ice (Davis et al. 2020) and, over the long-term, shape biological communities according to their abilities and adaptations to low ambient DO conditions (Magnuson et al. 1985). With oxygen depletion, microbial metabolism shifts to other electron-acceptors, modifying the partitioning and concentrations of major elements (N, C, S, P, Fe) under the ice, with potentially far-reaching consequences for the following open water season (Gammons et al. 2014; Kincaid et al. 2022). While climate warming is expected to result in significant modifications of the DO dynamics under lake ice, studies insofar have reached divergent conclusions on whether climate change shall limit or instead reinforce the duration and vertical extent of hypoxia under the ice. For instance,

climate warming was observed or expected to promote oxygenation under ice in some cases, (Flaim et al. 2020; Smits et al. 2021) but predicted to extend the duration of hypoxia under the ice for others (Golosov et al. 2007; Couture et al. 2015).

Schematically, the dynamics and duration of bottom hypoxia under lake ice depend on three variables: the ice-cover duration, the DO stock at the ice onset, and the rate of DO decay under the ice (Terzhevik et al. 2009); all of which are susceptible and expected to vary with climate warming. A shorter ice cover reduces the time over which hypoxia can develop and persists (Smits et al. 2021). Besides, climate warming affects water temperatures and mixing duration in fall (Råman Vinnå et al. 2021), both influencing DO stocks at the ice onset (Flaim et al. 2020). The DO decay rates are also likely to respond to climate change, potentially through biogeochemical but also physical pathways. For instance, DO decay under the ice primarily arises from the sediment oxygen uptake (SOU; Bengtsson and Ali-Maher 2020), i.e., the diffusion of oxygen within the sediment where it is consumed by both the aerobic mineralization of sediment organic matter (OM) and the abiotic oxidation of reduced solutes produced by anaerobic microbial metabolism (Müller et al. 2012). The oxygen consumption in the sediment increases with the sediment content in OM (Müller et al. 2012), so that a greater SOU is expected in situations where climate warming results in greater OM exports to the sediment (Steinsberger et al. 2017), either through enhanced lake primary production (Preston et al. 2016) or greater terrestrial OM inputs (Couture et al. 2015). Yet, DO decay might not be solely biogeochemically controlled. In the first investigations of under-ice dynamics, DO decay rates were already observed to increase with the warming rate of deep waters by sediment heat release (Mortimer and Mackereth 1958), an association confirmed by more recent studies (Golosov et al. 2007; Terzhevik et al. 2009). Although the processes tying the sediment heat release to DO decay remain to be identified, sediment heat content is another pathway by which climate warming might modify DO decay under lake ice (Fang and Stefan 1996; Golosov et al. 2007).

Because of the diversity of involved processes contributing to the DO dynamics and the climate factors acting upon them, there is no single scenario for the effect of climate warming on DO under lake ice. The different components of the DO dynamics can respond synchronously and sometimes through divergent pathways to climate warming. For instance, a modeling approach applied to the boreal Lake Langtjern suggested that despite an earlier ice break up, DO under ice is likely to decrease due to greater climate-driven dissolved organic carbon inputs from the catchment (Couture et al. 2015). Therefore, shifts in the extent and degree of hypoxia in ice-covered lakes due to climate change are case-specific.

Processes of DO decay in high altitude lakes, where deep-water hypoxia can develop over the course of the 6–9 months

of ice cover despite low productivity, are even less understood (Smits et al. 2021). Compared to the low elevation temperate and boreal lakes, their high-altitude counterparts are less prone to summer hypoxia since the absence or short duration of summer stratification limits deep deoxygenation during the open water season (Perga et al. 2018; Granados et al. 2020). However, high-altitude lakes are exposed to amplified climate warming (Gobiet et al. 2014) to which they commonly respond by a later ice-on and an earlier ice-off (Parker et al. 2008; Brown and Duguay 2010; Preston et al. 2016; Smits et al. 2021), and possibly by a longer fall mixing (Flaim et al. 2020). The consequences of climate warming on hypoxia duration during wintertime remain unclear as the outcome would depend on the relative importance of ice duration, DO stocks at ice onset and DO decay rates in controlling near-bottom DO under the ice.

Here we present a comprehensive database of high-temporal resolution time series of DO concentration and temperature across 14 mountain lakes located in the French Alps, joined with a set of attributes for the lakes and their catchment. First, we quantified the duration of hypoxia spatially, i.e., among lakes, and temporally, i.e., among years within lakes. We then identified which of ice phenology, DO concentrations at the ice onset or DO decay rate was the main driver of hypoxia duration. As DO decay rate stood out as the dominant predictor of hypoxia duration, we evaluated, in a second step, the relative contribution of the biogeochemical and physical controls to DO decay rates. In the final step, we proposed a simple mechanistic model as a proof-of-concept of the mechanisms derived from the data analysis.

Materials and methods

Study sites and monitoring setup

The studied lakes are part of the observatory of the Sentinel lakes network (http://www.lacs-sentinelles.org/, last accessed February 2021, Birck et al. 2013). The network developed a set of standardized protocols adapted for long-term monitoring of mountain lakes, accounting for their remoteness and extreme conditions. The protocols rely on high-frequency monitoring from autonomous sensors and one annual field campaign in early September to maintain the sensors, download the data, and perform vertical profiling, Secchi depth measurements, and water sampling. Fourteen of these lakes are considered in the analysis and classified as dimictic or cold monomictic (Fig. 1, Table 1).

The monitored lakes span the French Alps, from the foot-hill of the Mont Blanc down to the Southernmost part of the Alps (Fig. 1), with altitudes ranging from 1945 to 2752 m above sea level (Table 1). They are small lakes with surface areas and maximum depths (z_{max}) that vary over one order of magnitude (from 1 to 16 ha, 7 to 50 m deep). Drainage ratios (catchment to lake surface areas) range from 9 to 130. All lakes are oligotrophic, poorly productive, and ice-covered for

150–230 d of the year. Despite a narrow range of altitudes, the lake catchments are highly variable in terms of vegetation coverage (Normalized Difference Vegetation Index [NDVI] from 0 to 0.7) and proportions of cryogenic features (glaciers and permafrost from 0% to 73% and 0% to 94%, respectively).

As part of the monitoring protocols, all lakes are equipped with autonomous temperature sensors (Tinytag® or Hobo Water Temperature Pro v2®, accuracy ± 0.5 °C) 2 m below the surface, along with a temperature-DO sensor (PME Minidot, accuracy ± 0.1°C and ± 0.3 mg O_2 L^{-1}) placed 1 m above the sediment and anchored to a submerged buoy at the maximum lake depth. Both water temperature and DO concentration were recorded at 1-h intervals. Twenty-one DO and water temperature data series were available.

DO dynamics

Since no direct ice measurements were available, the ice-cover phenology was estimated from high-frequency near-surface and near-bottom water temperatures. The date of ice-on was defined as the time when lake bottom temperature reached a local minimum after the fall cooling, i.e., the moment when the water column suddenly isolates from the atmosphere and the inverse thermal stratification, resulting from a coupled effect of heat loss and sediment heat release, becomes a distinctive feature of under-ice waters (Fang and Stefan 1996). The date of ice-off was defined as the time when the near-surface water temperature was rising after ice-on by more than 0.1°C day^{-1}, i.e., the moment when the water column gets in contact with the atmosphere and warms up (SI 1). We acknowledge that the quantification of the ice cover phenology is subject to arbitrary choices but keeping consistent metrics throughout the study ensures that trends are conservative among sites and years.

DO_{init} was computed as the near-bottom DO at the determined date of ice on. Time to hypoxia corresponded to the number of days to reach DO = 2 mg L^{-1} after the date of the ice onset. The hypoxia duration was computed as the number of days for which the near-bottom DO ≤ 2 mg L^{-1} after the ice onset and before the determined ice-off.

In earlier studies, under-ice DO depletion had been modeled from either a zero- or a first-order kinetics. Zero-order kinetics model the DO dynamics as a linear decrease over time, computed over the first weeks after ice onset or in-between changepoints in the DO time-series (Obertegger et al. 2017; Granados et al. 2020; Smits et al. 2021). A zero-order model assumes a substrate limitation of DO consumption which, close to the lake bottom (Beutel 2003), might be better adapted to model the oxidation of reduced compounds released from the sediment (Müller et al. 2012). In contrast, first-order kinetics (Golosov et al., 2007, Terzhevik et al. 2009) model the DO dynamics as an exponential decay that better reflects diffusion-limited processes at the sediment–water interface (Beutel 2003), i.e.,
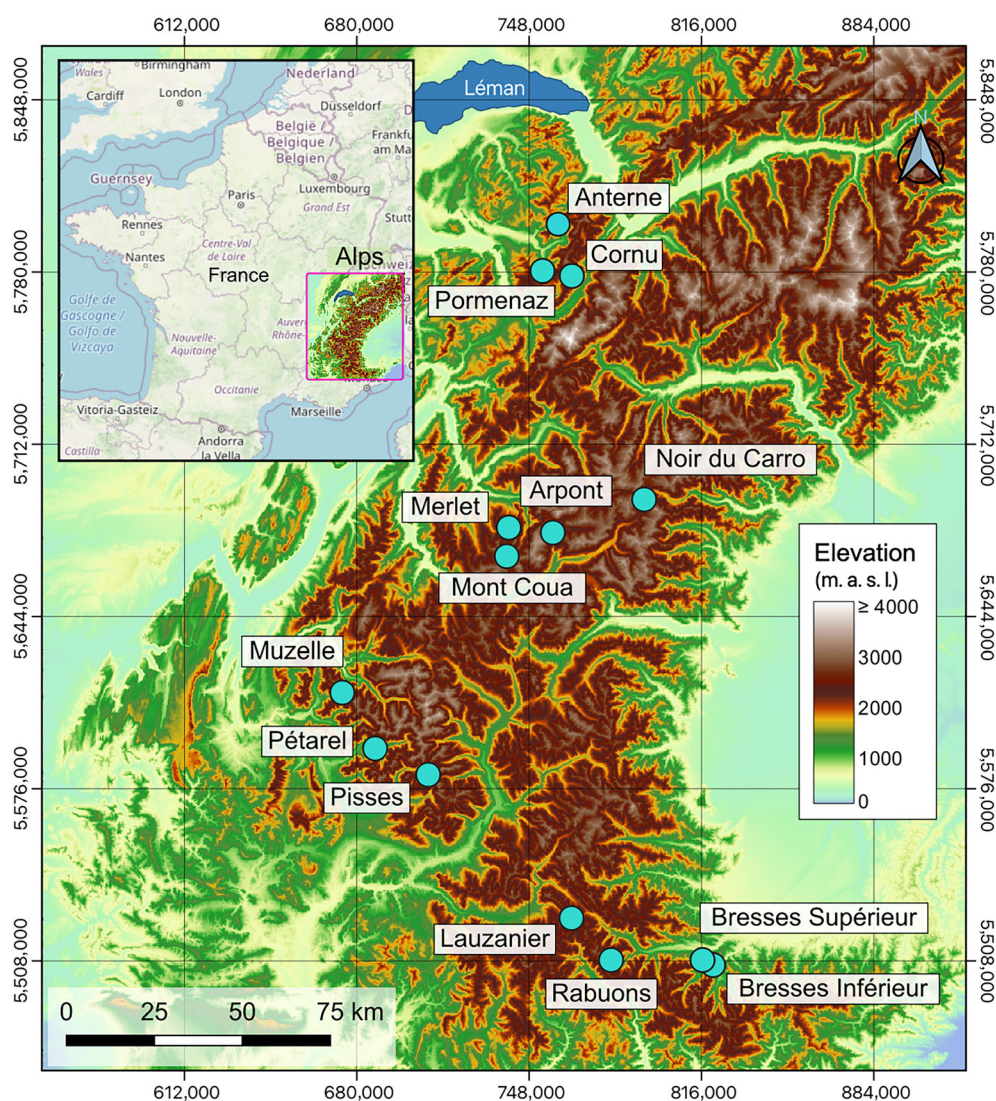
Fig. 1. Locations of the 14 monitored alpine lakes, distributed across the French Alps.

$$DO(t) = DO_{init} \times e^{-K_{exp} \cdot (t - t_0)}$$

where t_0 is the determined ice-on (t is expressed in days), DO_{init} is the initial DO concentration. K_{exp} is the exponential decay coefficient that is fitted to the data. We opted for the exponential decay model as it fitted better, was the most consistent across lakes, but also over time as it reproduces the asymptotic trend as DO gets closer to 0 mg L^{-1}. Conclusions were however independent of the type of model used to simulate the DO dynamics under ice.

In several cases, near-bottom DO first increased for several days after ice-on, likely due to residual light penetration through the ice allowing either under-ice primary production (Granados et al. 2020), or due to buoyancy-driven downslope flows (Ulloa et al. 2019). To minimize this bias, the decay models were fitted on the DO time series starting after the local DO maximum was reached. The length of the fitting window was manually adapted

in the case of two lakes, where the observed DO patterns showed complex features. This was the case in Lake Bresses Inférieur during the winter of 2018–2019, where DO followed an exponential decay for 50 d after ice-on with significant unexplained upward deviations afterwards. The curve-fitting was conducted over the first 50 d after ice-on in this case. In Lake Merlet Supérieur, DO measurements presented an abrupt increase 100 d after ice-on and K_{exp} was fitted to the data recorded before this event. Overall, fitting performances were statistically robust, with determination coefficients $r^2 > 0.83$, and a mean r^2 of 0.93 across all lakes and years.

Explanatory variables

We investigated the relationships existing between DO dynamics under ice and potential predictors describing lake morphology, thermal stratification at ice-onset (i.e., cryoregime), lake productivity, and the warming rate of deep

Table 1. Main geographical attributes for 14 alpine lakes and their respective catchments.

Lake	Mixing regime	Altitude [m a.s.l.]	Area [ha]	z_{max} [m]	Secchi depth [m]	Drainage ratio [unitless]	Catchment NDVI [dl]	Macrophyte coverage [%]	Monitored winters (n)
Anterne	Dimictic	2063	11.1	12	3.6–10.0	21	0.60	9	2015–2019 (4)
Arpont	Cold monomictic	2666	3.7	17	0.5–0.9	91	0.02	ND	2018–2019 (1)
Bresses inférieur	Dimictic	2458	1.2	13	6.0–9.0	9	0.35	ND	2018–2019 (1)
Bresses supérieur	Dimictic	2501	1	12	5.0–7.0	36	0.20	ND	2018–2019 (1)
Cornu	Dimictic	2276	6.4	22	10.0–13.0	10	0.37	0	2018–2019 (1)
Lauzanier	Cold monomictic	2284	3.8	7	7.0	130	0.34	30	2017–2019 (2)
Merlet	Dimictic	2452	4.9	29	7.6–13.3	13	0.40	6	2018–2019 (1)
Mont Coua	Cold monomictic	2672	2.5	10	3.8–4.1	32	0.14	ND	2018–2019 (1)
Muzelle	Dimictic	2105	9.7	18	0.6–8.0	46	0.24	<1	2014–2015; 2018–2019
Noir du Carro	Cold monomictic	2759	1.2	11	10.0–11.3	41	0.16	0	2018–2019 (1)
Petarel	Dimictic	2095	2.5	20	11.6–13.5	53	0.44	0	2018–2019 (1)
Pisses	Cold monomictic	2490	1.7	7	7.5–8.0	47	0.44	ND	2017–2019 (2)
Pormenaz	Dimictic	1945	4.4	9	5.7–8.4	11	0.71	10	2018–2019 (1)
Rabuons	Dimictic	2500	16.3	50	11.5–13.5	19	0.19	<1	2017–2019 (2)

waters. Morphological descriptors were lake depth and lake photic ratio; the latter being defined as the ratio of light penetration depth in water to the maximum lake depth. The lake photic ratio ($phot_{ratio}$) was compiled for each year such as,

$$phot_{ratio} = \frac{z_{eu}}{z_{max}}$$

with the euphotic depth $z_{eu} = 2.5 \cdot z_{Secchi}$ (Joint Research Centre, Institute for Environment Sustainability 2012).

We characterized the lake cryoregime (i.e., cryomictic or cryostratified) as defined by Yang et al. (2021) from the mean temperature of the water column at ice onset (WTR_{ice-on}). Briefly, cryomictic lakes are shallow or wind-exposed lakes in which waters can mix and thus cool down to 0–1°C before ice forms. In cryostratified lakes, ice forms as soon as the surface reaches the freezing point, while deeper waters are 2–4°C (Yang et al. 2021). Lakes with WTR_{ice-on} in the range 0–1°C were classified as cryomictic, whereas lakes with WTR_{ice-on} above 2°C were classified as cryostratified (Yang et al. 2021).

Biogeochemically, the DO decay rate is expected to be greater in lakes with greater supplies of organic carbon (Leppi et al. 2016; Terry et al. 2017) from both autochthonous and terrigenous origins. In alpine lakes, Secchi depth alone is a poor predictor of pelagic productivity because water transparency strongly varies with the catchment sediment load (Olson et al. 2017; Perga et al. 2018). Considering that primary production is essentially littoral in small and clearwater oligotrophic lakes (Devlin et al. 2016), the percent macrophytes coverage was considered as a proxy for lake productivity. It was measured in August 2016 or 2017 in 25 quadrats regularly distributed on the lake area. Inputs of terrigenous OM and

catchment productivity were estimated using drainage ratios (Cremona et al. 2019), and the catchment vegetation cover (NDVI; Larsen et al. 2011), respectively. The NDVI values correspond to the mean peak productivity over 2013–2018.

The warming rate of deep waters was assessed through its e-folding timescale coefficient (K_{heat}), computed by fitting the near-bottom daily-averaged temperature measurements during the ice-covered period to the model $T_t = T_f - (T_f - T_0)e^{-K_{heat}(t-t_0)}$, where T_0 corresponds to the temperature measured at the time of ice-on, T_f at ice melt, and t is the time expressed in days after ice-on (t_0).

The relationships between DO decay rate coefficient, i.e., K_{exp}, and potential predictors were tested using linear regression models, with log-normalized data when necessary. Some lakes had records for multiple winters (Anterne, Lauzanier, Muzelle, Pisses, Rabuons), while some predictors (lake morphology, catchment land cover) were year-invariant. Weighting the contribution of lakes by the number of years of measurements ensured a balanced contribution of lakes to the final models. However, results did not vary between weighted and unweighted models.

Reaction–diffusion model

To assess the mechanistic processes linking predictors to DO decay in the field dataset, we used a simplified model of coupled DO and water temperature under the ice, set on a hypothetical alpine lake with a parabolic morphology of 20 m max depth (average max depth was 17 m in our dataset) and 5 ha surface area (average surface area was 4.8 m in our dataset). The modeling framework considers diffusion–reaction equations for temperature and oxygen. The model

solves the one-dimensional (vertical), diffusion reaction equation for horizontally averaged scalar field, $C(z,t)$ being either the DO or the T field

$$A(z)\frac{\partial C(z,t)}{\partial t} = \frac{\partial}{\partial z}\left(A(z)K(z,t)\frac{\partial C(z,t)}{dz}\right) + \frac{\partial A(z)}{\partial z}F$$

with,

- $A(z)$ the bathymetry;
- $K(z,t)$ the vertical turbulent diffusivity defined as a function of the buoyancy frequency (N^2): $K_z = aN^{-2b}$ (Jassby and Powell 1975; Heinz et al. 1990; Hondzo and Stefan 1993);
- F is the flux at slopping bottom ($\partial A/\partial z$). F is either the sediment heat flux or the sediment oxygen uptake:
  - Case DO: $F = -k_{DO}(DO(z) - DO_{SWI})$, with $k_{DO} = \frac{D_{DO}}{\delta}$, and $DO_{SWI} = \frac{DO(z)}{2}$ with D_{DO} the molecular diffusivity for DO, δ the constant diffusive boundary layer and DO_{SWI} the oxygen concentration at the sediment water interface (Müller et al. 2012; Bouffard et al. 2013).
  - Case T: $F = -k_T$, with $k_T = \frac{He^{-k_d z} e^{-\tau t}}{\rho C_p}$, with ρ, the water density, Cp, the heat capacity for water, τ, the decay time scale for sediment heat flux, k_d, the light extinction and H the sediment heat flux per unit area. Here the sediment heat flux decreases over time and depth.

The ice-water boundary is treated as a Dirichlet condition for temperature, $T(t, z = 0) = 0°C$, and as a no flux Neuman condition for DO, $\left(\frac{dC}{dz}\big|_{z=0} = 0\right)$. The lake bottom (i.e., deepest point) boundary condition is treated as no-flux Neuman condition for both T and DO (the flux at the bottom is already included in the last term of the equation). We stress that the equation is valid in the case of horizontally averaged constituents (Stepanenko et al. 2016). Full model specifications and parameters are provided in SI 2.

At ice onset, the DO concentration was considered uniform over depth, whereas the initial vertical temperature profile was determined by the respective cryoregime. The near-bottom (1 m above the sediment) DO decay rate was computed for different scenarios, testing for the effects of:

i. Cryoregimes, i.e., a cryomictic (well mixed water column at ice onset with temperature close to 0°C with a temperature increasing near-bed) and a cryostratified regime (temperature increase with depth close to the surface and well mixed conditions down to the bottom; Yang et al. 2021). Boundary conditions for water temperature were set at 0°C at the surface and 3°C at the lake bottom.

ii. Initial sediment heat release set at 0, 1, 2, and 4 W m^{-2}. Values for the initial sediment heat flux were determined based on simulations on a well-established bulk model FLake (Golosov and Kirillin 2010) for a lake of similar latitude and longitude as Lake Anterne with a light extinction coefficient ranging between 0.4 and 4 m^{-1} (i.e., Secchi depth within 0.5–5 m, comparable to the range found in

our dataset). Such values for the initial sediment heat release are in line with those reported in previous studies (Kirillin et al. 2012; Zdorovennova et al. 2021)

Results

Variability of under-ice DO dynamics across and within lakes

In all lakes, bottom DO decreased under ice, with total DO losses for the ice-on period ranging from 2.2 to 12.3 mg L^{-1} for Lakes Arpont in winter 2018–2019 and Pisses in 2017–2018, respectively. The duration of hypoxia was highly variable among lakes, from no hypoxia for Lakes Arpont 2018–2019, Muzelle 2018–2019 and Rabuons 2018–2019, to 236 hypoxic days for Mont Coua, where hypoxia occurred as early as 24 d after the ice onset (Figs. 2, 3a) and persisted a month beyond the ice-off. The duration of hypoxia was also highly variable among years for a single lake. For instance, Lake Muzelle experienced 0 d of hypoxia in 2018–2019 and 108 d in 2014–2015. In Lake Anterne, hypoxia duration ranged between 143 and 195 d over the 4 recorded winters.

The duration of hypoxia was neither correlated to ice cover duration (Fig. 3a), nor to DO saturation at the ice onset (DO_{init}, Fig. 3b). However, the duration of hypoxia among lakes and years was strongly dependent on the DO decay rate K_{exp} (Fig. 3c). Because the coefficient K_{exp} was, by far, the best predictor of hypoxia duration in our dataset, the subsequent analyses focused on uncovering the processes governing the DO decay rate in mountain lakes.

The DO decay coefficient K_{exp} ranged from 0.0016 to 0.0626 d^{-1}, i.e., e-folding decay timescales between 598 and 16 d, respectively. K_{exp} showed substantial variability among lakes, and among years for a single lake (Fig. 4a). Some lakes showed temporary breaks in the DO decay trends (for instance, Merlet supérieur, Muzelle in 2014–2015 and Bresses inférieur, Fig. 2). In the case of Bresses inférieur, hypoxia was reached 100 d later than expected from an exponential decay model (Fig. 4b). For all other lakes, the DO dynamics fell within the expected model describing time to hypoxia from K_{exp}, confirming that an exponential decay model explains the temporal evolution of DO in most lakes over the entire ice-covered period (Fig. 4b).

All lakes, except for Lakes Mont Coua and Lauzanier 2018–2019, had bottom water temperatures above 2°C at ice onset (Fig. 5), indicating that the majority of lakes in our dataset can be regarded as cryostratified (Yang et al. 2021). Lake Mont Coua, with bottom water temperature as low as 0.2°C at the ice onset, can unambiguously be classified as cryomictic. For Lauzanier, the cryoregime is somewhat uncertain as bottom water temperature were slightly lower than 2°C in 2018–2019, but not as low as could be expected for a strictly cryomictic lake (Yang et al. 2021). Nevertheless, the greatest K_{exp} was observed in the single

unambiguously cryomictic lake (Mont Coua, Fig. 5). With only one cryomictic lake in the dataset, we cannot robustly conclude on the potential effect of cryoregime on DO decay K_{exp}. As the cryomictic lake appeared as an outlier in our dataset, we analyzed the predictive power of environmental variables for cryostratified lakes only. Note that when the dataset was restricted to cryostratified lakes only (including Lauzanier 2018–2019), K_{exp} remained the best predictor for hypoxia duration ($r^2 = 0.67$, $p < 10^{-5}$), far above initial DO ($r^2 = 0.11$, $p = 0.24$) and ice duration ($r^2 = 0.08$, $p = 0.23$).

Predictors of under-ice DO decay rates for cryostratified lakes

Figure 6 summarizes the predictors of under-ice DO decay rates for cryostratified lakes. K_{exp} was negatively correlated with lake depth (Fig. 6a), although the determination coefficient from linear regression was relatively low (28%, Table 2). K_{exp} increased significantly with the photic ratio at the end of summer (Fig. 6b), following a linear relationship and providing the greatest coefficient of determination (59%, Table 2). K_{exp} was positively correlated to the deep warming rate under the ice (K_{heat}), which was a better predictor of K_{exp} (Fig. 6c) than any of the variables used as OM supply proxies (i.e., drainage ratio, NDVI and macrophyte

cover, Fig. 6d–f). K_{heat} explained up to 33% of K_{exp} variability.

Diffusion–reaction model simulations

Field data suggested that the lake cryoregime and the e-folding coefficient for deep warming, i.e., K_{heat}, were likely to affect K_{exp}, which we investigated further using model simulations. Specifically, the model considers the initial cryoregime and resolves the vertical temperature and DO evolution based on heat release from sediment interface and irreversible vertical diffusive fluxes across the water column. Reported K_{exp} are those simulated 1 m above the sediment. In this hypothetical lake mechanistic model, the cryoregime had a significant influence on K_{exp}, with values about 25% higher in a cryomictic lake compared to a cryostratified lake, in the absence of any sediment heat release (Fig. 7a). K_{exp} increased along with a greater sediment heat release in the cryostratified regime, while K_{exp} sensitivity to sediment heat flux was extremely low in the cryomictic lake (Fig. 7a). The vertical temperature profile revealed that the near-bed stratification, that already existed at the ice onset, persisted under the ice of the cryomictic lake, even in the absence of sediment heat release (Fig. 7b). Sediment uptake drew down DO from the bottom layer only (up to 2–3 m above the sediment), and, as
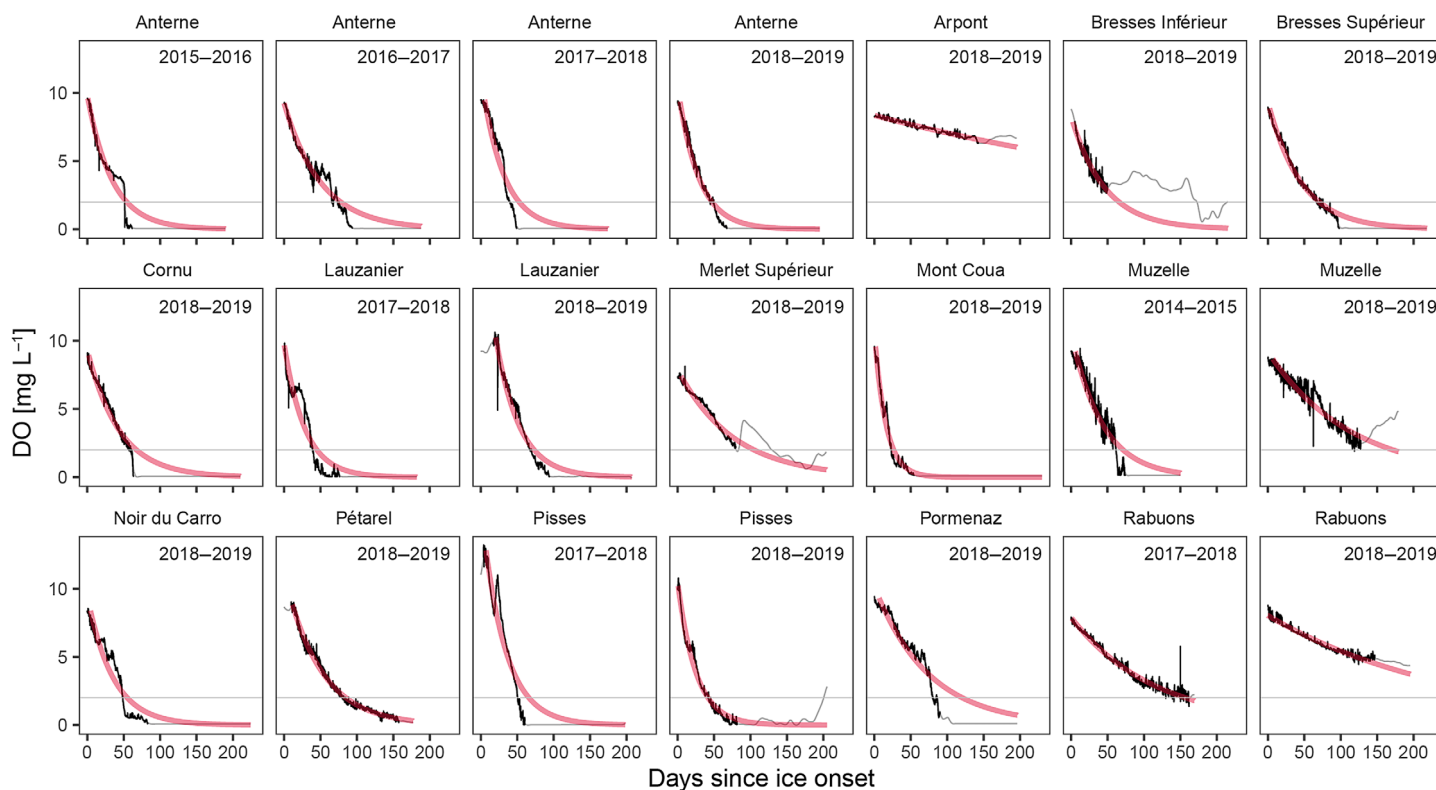

Fig. 2. Patterns of near-bottom (1 m above the sediment) DO concentration, shown both as measured (thin black lines) and fitted (thick red lines), during the under-ice period in the 14 studied lakes. The darker part of the thin lines indicates the data used for curve-fitting and computation of K_{exp} coefficients. The threshold for hypoxia (2 mg L^{-1}) is indicated by the horizontal gray line.
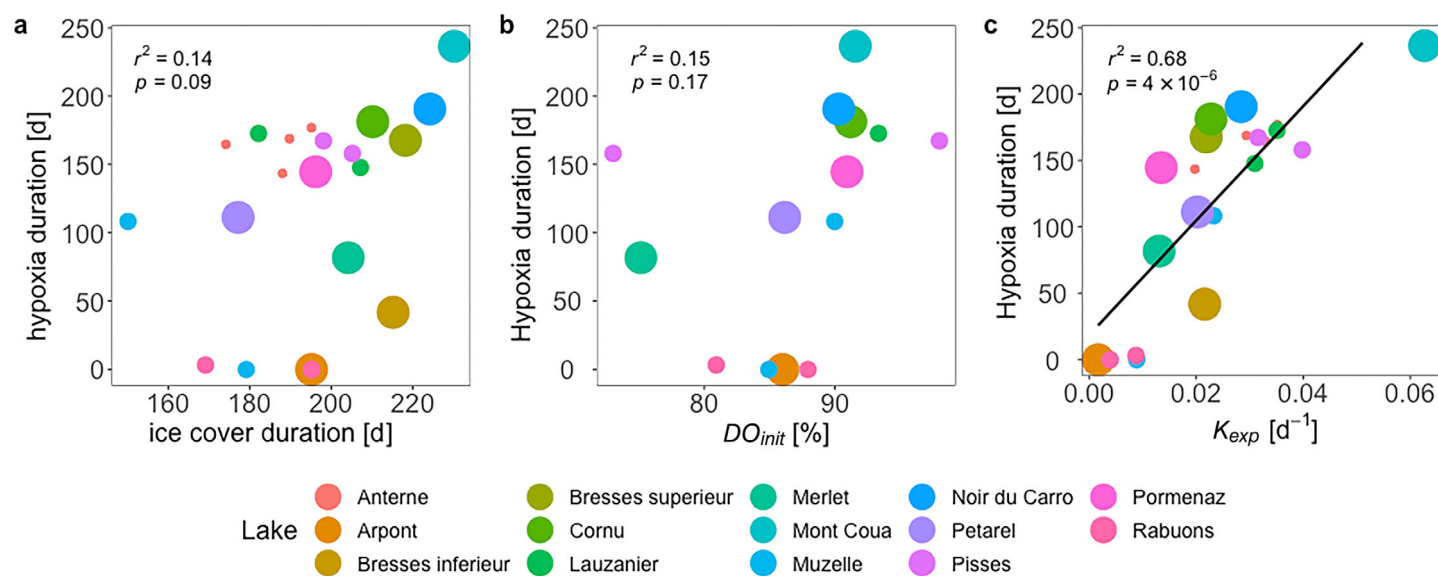
Fig. 3. Relationships of bottom hypoxia duration under the ice and (**a**) the ice cover duration, (**b**) the initial near-bottom DO at ice-onset, and (**c**) the DO decay coefficient K_{exp}. For Lake Mont Coua, the spring mixing occurred a month later than the ice melt, so that the hypoxia duration exceeds the ice cover duration (SI 1). The size of data points is proportional to the weight given within the linear model (*see* Materials and methods).

the near-bed density gradient prevented DO diffusion and resupply from the above layers, resulted to a greater near-bottom DO depletion in a cryomictic regime (Fig. 7d). Because of the persistence of near-bed stratification, DO depletion was similar irrespective of the sediment heat flux for a cryomictic lake (Fig. 7a). In the cryostratified regime, the vertical temperature

profile remained homogenous below the 14 m depth in the absence of sediment heat release (Fig. 7c) so that the downward DO diffusion in the water column partly compensated for sediment uptake. The near-bottom DO decay was limited in the cryostratified regime when sediment heat release was absent (Fig. 7e). With greater sediment heat release, a near-bed
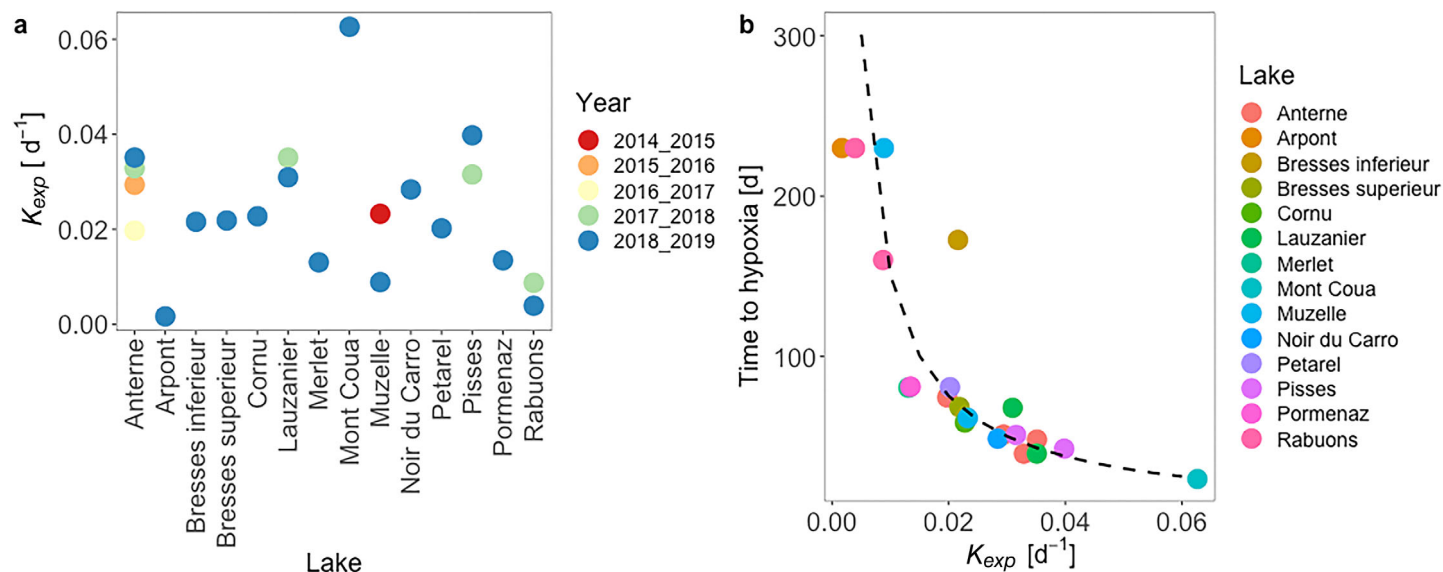

Fig. 4. (**a**) DO decay rate coefficient K_{exp} for all lakes (x axis) and years (colors). (**b**) Relationship between observed K_{exp} and time (in days) for lakes to reach near bottom hypoxic conditions, i.e., DO $\leq$ 2 mg L^{-1}. Data points represent the observed time to hypoxia after the onset of ice in days. The dotted line represents the theoretical first-order differential equation model estimating the time to hypoxia $\tau_{hypoxia}$ based on observed K_{exp}, such that $\tau_{hypoxia} = K_{exp}^{-1} \log\left(\frac{DO_{init}}{DO_{hypox}}\right)$, with DO_{hypox} the threshold for hypoxia, set at 2 mg L^{-1}, and assuming DO_{init} = 9 mg L^{-1} (the mean value of the dataset). For lakes that never reached hypoxia, the time to hypoxia was set at 230 d (the longest ice duration).
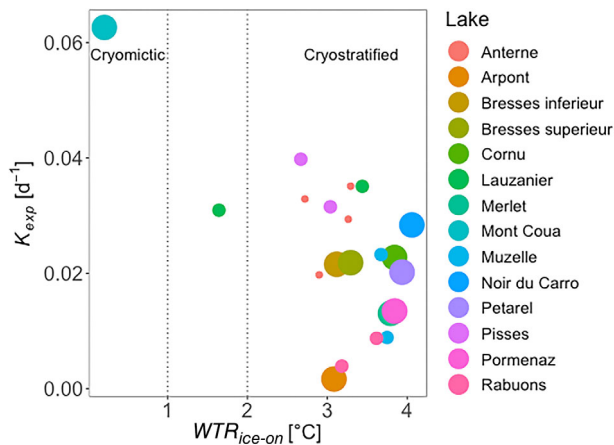
Fig. 5. DO decay rate K_{exp} and cryoregimes classification based on mean water temperature in the water column at ice-on. Lake Mont Coua was the only unambiguously cryomictic lake in our dataset.

temperature gradient developed under the ice of the cryostratified lake (Fig. 7c), reducing DO downward diffusion from the upper layers and leading to faster DO decay near the bottom (Fig. 7e).

Discussion

Our extensive dataset revealed highly variable near-bottom DO dynamics under the ice of alpine lakes. The rate of DO decay K_{exp} was the most critical parameter for development of near-bed hypoxia. The value of K_{exp} allowed confident prediction of the time required to reach near-bottom hypoxia as well as of the duration of hypoxia under ice. The DO decay rate was twice as high for the cryomictic lake as compared to the other, cryostratified, lakes, suggesting that the lake cryoregime could influence the DO dynamics under the ice. The DO decay rate among cryostratified lakes varied mainly with light climate (i.e., the photic ratio). The statistical analyses
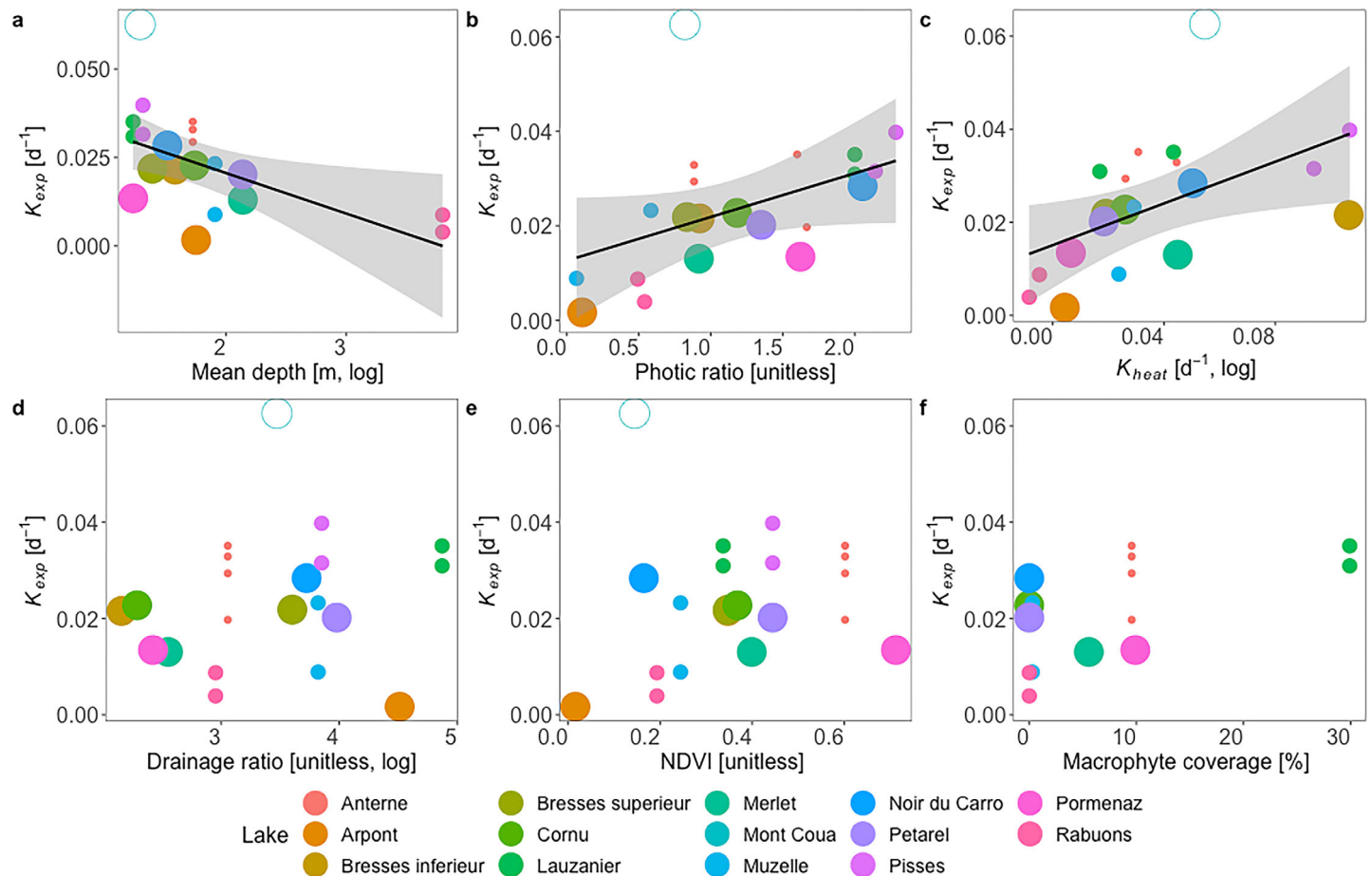

Fig. 6. Exponential decay coefficients K_{exp} (per day) as a function of the potential predictors, i.e., (**a**) mean lake depth, (**b**) the photic ratio, (**c**) deep warming rate at the lake near-bottom, (**d**) lake drainage ratio, (**e**) catchment vegetation cover, NDVI, and (**f**) lake relative macrophyte coverage. Linear fits are performed only over cryostratified lakes (closed points), while the cryomictic lake (open point) data is indicated only for a comparative purpose. The size of data points is proportional to the weight given within the linear model.

Table 2. Linear model results (determination coefficient r^2 and associated *p*-value) for K_{exp} and the selected variables for the cryostratified lakes.

Predictors	Variable (transformation; unit)	r^2	*p*-value
Bathymetry	Mean depth [log; m]	0.28	0.01
Photic ratio	$phot_{ratio} = z_{eu}/z_{max}$ [unitless]	0.59	6×10^{-5}
Organic matter supply	Drainage ratio [log; unitless]	0.03	0.49
	NDVI [log; unitless]	0.12	0.12
	Macrophyte coverage [%]	0.22	0.07
Sediment heat release	Warming rate under the ice, K_{heat} [log; d^{-1}]	0.33	8×10^{-3}

indicated a strong relationship tying the DO decay rate K_{exp} to the deep warming rate K_{heat}, thus pointing, for cryostratified lakes, to a key role of the sediment heat release on the DO dynamics under ice. A testbed model explored whether differences in the near-bed stratification could be the mechanism by which K_{exp} depended on varying deep warming rates under the ice but also potentially on the lakes cryoregimes.

Modeling the DO dynamics under the ice

Near-bottom DO decreased after ice-on, with a high depletion rate over the first days and weakening as the ice-on period progressed, consistently with the observations by Terzhevik et al. (2009) and Smits et al. (2021). The high-resolution monitoring of near-bottom DO also revealed episodes of complex patterns and deep oxygen resupply that caused DO evolution to diverge from an exponential decay. On two occasions (in Bresses inférieur and Merlet), the disruptions in DO patterns forced us to limit the fit of the exponential model to the period prior to DO disruption. Investigating whether disruptions in the exponential DO decay arise from technical aspects (vertical shift of the mooring position) or physical processes (e.g., under-ice convection, snow-melt, or ice or snow subsidence) would require additional data such as light, pressure and weather data (Smits et al. 2021), that were not available in this study. However, DO decay resumed quickly after temporary episodes of oxygen resupply, and the exponential DO decay model, even when computed only from a part of the dataset, fitted well with the observation throughout the iced season for all but one lake: for Bresses Inferieur, the temporal trajectory deviated clearly from an exponential curve after about 50 d. The time to reach hypoxia lagged by 100 d compared to what could be predicted from K_{exp} computed over the first 50 d. The disruption in DO dynamics in Lake Bresses Inférieur coincided with a complex thermal dynamic of the water column from day 50 due to the intrusion of colder water at the lake bottom (SI 1), pointing to a resupply of oxygen likely due to groundwater inflows rather than episodic surface events.

The predominant DO decay dynamics in all lakes and years throughout winter confirms that the Winter stage I sensu Kirillin et al. (2012), i.e., snow-covered ice, is the most

common model for the iced season of high-altitude mountain lakes, echoing conclusions from Smits et al. (2021). In such conditions, K_{exp}, the exponential DO decay rate, appears as a handy universal metric to quantify, compare and model the near-bottom DO dynamics throughout the ice-cover season. The duration of hypoxia under ice was much more strongly dependent on DO decay rate K_{exp} than on ice duration or initial DO concentrations, and the time to reach hypoxia was accurately predicted from K_{exp}. Addressing the drivers of K_{exp} variability among and within lakes and the processes governing DO decay is key to predicting under-ice near-bottom hypoxia for alpine lakes, for current conditions and under future climate change.

Physical controls of DO decay under the ice

K_{exp} varied by more than one order of magnitude among lakes and by a factor 1.8 among years for the lake represented by more than 2 yrs in the dataset (Lake Anterne). In our study, linear rates of change computed in the first weeks after the ice onset were, on average, equivalent to 0.11 mg L^{-1} d^{-1}, except at Lake Mont Coua, where it was 0.30 mg L^{-1} d^{-1}. These values are well within the reported range of 0.10–0.40 mg L^{-1} d^{-1} found at the bottom of other high-altitude lakes (Granados et al. 2020; Smits et al. 2021) or low-land oligotrophic lakes (Ghane and Boegman 2023). The high spatial variability in K_{exp} was less surprising than its temporal variation considering the already well-observed influence of lake morphology on the DO dynamics under ice (Mathias and Barica 1980; Leppi et al. 2016). The DO decay rates are typically faster in shallower lakes under ice (Mathias and Barica 1980; Leppi et al. 2016) as a result of a greater contribution of sediment processes to the water column conditions, i.e., greater sediment surface to water volume ratio (Bengtsson and Ali-Maher 2020).

Sediment oxygen uptake, which is ultimately the process driving DO consumption under ice, is expected to increase along with the sediment OM content and therefore with lake productivity (Steinsberger et al. 2017). However, surprisingly, the values of K_{exp} in the poorly productive lakes of this study were of the same order of magnitude as those observed in the mesotrophic, organic-rich Lake Vendyurskoe in Russia (Terzhevik et al. 2009). Furthermore, K_{exp} did not vary along with estimators for OM inputs to the sediment. Although proper data on sediment OM would be necessary, our study points to SOU rates having a second role in explaining the variability in K_{exp} within and among the study lakes. The variability of the near-bed DO dynamics that we observed among and within lakes primarily arises from physical processes rather than changes in biogeochemical rates. Our results point to a crucial role of sediment heat release, and more broadly to the key role played by the near-bed stratification in modulating the rate of DO decay under the ice of low-productivity mountain lakes.
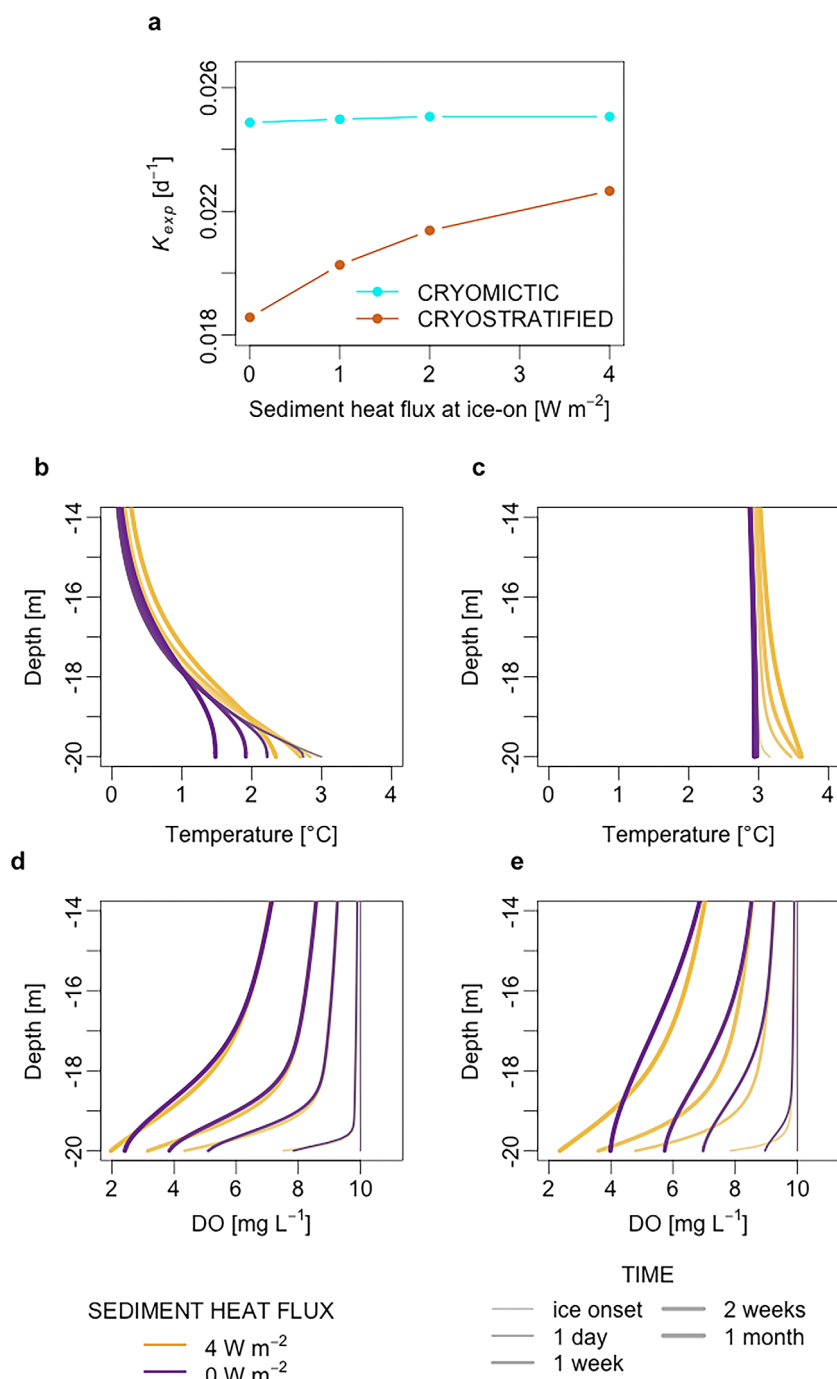
Fig. 7. (**a**) Effect of the cryoregime and sediment heat flux at ice-on (i.e., release) on K_{exp} at 1 m above the sediment for a 20 m deep lake. (**b–c**) Changes in the deep water temperature (14 m depth to the bottom) from the ice onset to the first month of ice cover for a cryomictic (b) and cryostratified (c) lake for a null sediment heat flux (purple) or a sediment heat flux at ice onset of 4 W m^{-2} (yellow). (**d** and **e**) Changes in the deep water DO for a cryomictic (d) and cryostratified (e) from the ice onset to the first month of ice cover for a null sediment heat flux (purple) or a sediment heat flux at ice onset of 4 W m^{-2} (yellow).

Linking near-bed stratification to DO decay through a testbed model

In cryostratified lakes, DO decay was significantly faster in lakes with higher deep warming rates. For the cryostratified

Lake Anterne, for which we had 4 yrs of monitoring, K_{exp} varied significantly among years, where K_{exp} increased 1.8-fold for a tripling of K_{heat}. Our results align with the observations of Mortimer and Mackereth ([1958](#)) and simulations by Golosov

et al. ([2007](#)) and Terzhevik et al. ([2009](#)), theorizing a mechanistic link between the deep water warming from sediment heat release and DO dynamics under ice. Using a reaction–diffusion model, we provided a proof of concept that near-bed stratification (i.e., near-bottom density gradient) generated by sediment heat release can produce different DO decay rates by limiting DO diffusion from upper water layers.

Our proof-of-concept does not exclude other mechanisms that have been previously proposed, but not yet formally proven, to underlie the relationships between DO decay rate and sediment heat. For instance, we did not account for heat or salts advection from downslope flowing currents (Golosov et al. [2007](#); Terzhevik et al. [2009](#); MacIntyre et al. [2018](#)), all of which should nevertheless reinforce the near-bottom density gradient. Downslope currents could also complexify the picture if they result in significant cross-shore advection, which has been observed but not yet quantified (Stefanovic and Stefan [2002](#); Ramón et al. [2021](#)). Nor did we include the suggested temperature-dependency of DO gradient within the sediment (Golosov et al. [2007](#)) due to the lack of observations to build upon. Although greatly simplified, the model provides evidence that the strength of stratification near the lake bottom, resulting from varying heat sediment release among lakes or years, can significantly contribute to the near-bottom oxygen dynamics by modulating DO vertical diffusion.

The K_{exp} observed for the cryomictic lake stood out from the whole dataset, reaching a value that was twice as large as those observed for cryostratified lakes of similar depth. Our simulation results also suggest that near-bed stratification could explain the greater DO decay rates observed in cryomictic lakes compared to all other cryostratified lakes. Cryomictic and cryostratified lakes differ in their depth-averaged ice-on temperatures and strength of the inverse stratification under the ice (Yang et al. [2021](#)). For cryostratified lakes, low wind exposure in fall restricts the heat loss to the water surface, until the surface reaches the congelation point (Yang et al. [2021](#)). The temperature and thereby density gradient of the inverse stratification is located close to the surface. In contrast, cryomictic lakes are exposed to wind mixing so that a much thicker water layer has to lose heat before the surface reaches the freezing point (Yang et al. [2021](#)) and the temperature gradient is much closer to the bottom. A strong near-bed temperature gradient occurs in cryomictic lakes regardless of sediment heat release, with strong consequences on the DO diffusive fluxes and thereby K_{exp}. The proposed physical model suggests a critical role of lake cryoregimes on under-ice DO dynamics, calling for observational field confirmation.

Physical controls of DO decay under ice and the light climate of open waters

Our results indicate that the summer light regime is a critical predictor of oxygen dynamics under the ice of cryostratified lakes. Specifically, the photic ratio (measured in the summer season) was the best predictor of oxygen decay

under ice. As sediment heat release is important for DO decay rates, the factors controlling sediment heat accumulation during open waters, such as light climate, indirectly control DO dynamics under ice (Golosov et al. [2007](#)). Sediment heat accumulation depends on water transparency (Fang and Stefan [1996](#)) and lake hypsometry, constraining the area of sediment directly exposed to solar irradiance. The photic ratio, measured at the end of summer, varies significantly among lakes and years, with photic depths as shallow as 5% of the maximum lake depth for lakes receiving glacial flour (Arpont, Muzelle for 2018–2019) and as deep as 220% of the maximum depth for the clearest ones (Noir du Carro, Pisses). Light penetration down to the bottom during summer generates weak density stratification with a greater heat accumulation in the sediment. In contrast, sediment heat accumulation will be restricted to the shallower sediments in more turbid lakes when more stable stratified waters prevent downward heat penetration (Fang and Stefan [1996](#)). Lakes of greater photic depth might have accumulated considerable amounts of heat in summer, and indeed we found a positive correlation between the lake photic ratio and K_{heat} ($r = 0.44$, $p = 0.04$). Greater sediment heat storage in summer generates a stronger near-bed density gradient when heat is released under the ice (Golosov et al. [2007](#)), causing, ultimately, a faster DO decay at the lake bottom during the ice-covered period.

DO under the ice of alpine lakes and climate change

In our study lakes, both the time to reach hypoxia and the duration of hypoxia under ice could be predicted well from the DO decay rate itself varying primarily, for cryostratified lakes, with the photic ratio. Ultimately, the combined lake depth and water transparency could also very well explain the
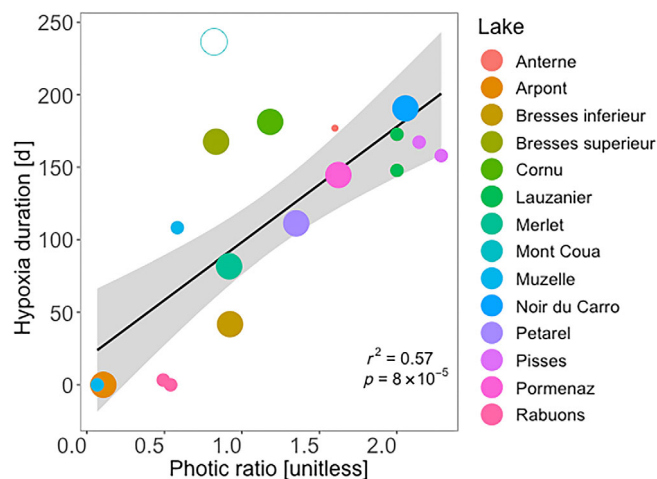

Fig. 8. Hypoxia duration (in days) as a function of the photic ratio (open symbol = cryomictic, closed symbols = cryostratified). The linear fit is performed for cryostratified lakes only. The equation of the linear model is Hypoxia_duration = 69.7 Photic_ratio + 20.5. The size of data points is proportional to the weight given within the linear model.

variability in the duration of hypoxia among and within lakes (Fig. 8), providing a framework through which the effect of climate change on the under-ice DO dynamics of alpine cryostratified lakes can be theorized.

While reduced in duration, the ice cover of lakes in the European Alps at altitude above 1500 m asl is predicted to persist until the end of the century even in the worst-case climate scenarios (Råman Vinnå et al. 2021). We expect changes in the duration of hypoxia under the ice to be more drastic in the shallowest lakes, although the magnitude might be case-specific. While the water transparency of mountain lakes is expected to undergo significant changes under climate warming (Parker et al. 2008), those changes are not expected to be monotonic, but rather dependent on the specific landscape features (Olson et al. 2017). Water transparency in mountain lakes responds mainly to catchment inputs in turbidity (for glacially-fed lakes) and colored dissolved organic matter (CDOM, for non-glacially-fed lakes). With glacier retreat, lakes get progressively disconnected from glacial inputs, leading to a turbidity of glacial-fed lakes that decreases and gets more variable in time (Olson et al. 2017; Olson et al. 2020). As disconnection gets complete, lakes suddenly shift from turbid to clearwater with substantial consequences on the heat content and vertical distribution in summer (Perga et al. 2018). Assuming a stable cryostratified regime, and a Secchi depth of 0.5 m for turbid glacial-fed lakes (as of Arpont and Muzelle 2018–2019) and 5 m for a non-glacially fed lake, a full glacial disconnection shall lead to hypoxia lasting 53 d longer in a 10 m max depth lake, and 21 d longer in a 30 m depth lake (based on Fig. 8). In both cases, this predicted lengthening of hypoxia is of similar scale and may outcompete the predicted reduction of ice cover for high altitude lakes of the Alps by the end of the century for the RCP2.6 scenario (20 d, e.g., Råman Vinnå et al. 2021). Hypoxia duration under the ice might remain steady or potentially increase under the ice of lakes getting disconnected from glacial waters in the future.

For alpine lakes that are currently non-glacially-fed, or for those that will lose glacial connection, CDOM controls diffuse light attenuation (Olson et al. 2017). Catchment greening (Carlson et al. 2017) is expected to promote CDOM exports to lakes (Olson et al. 2017). However, CDOM absorbs mainly in the UV domain, so that PAR attenuation does not scale to CDOM concentrations in the range of values observed for mountain lakes (Olson et al. 2017). On top, neither the lake Secchi depth nor the photic ratio were related to the catchment NDVI in our dataset, highlighting that the relationship between light climate and catchment productivity is far from direct in alpine lakes. Increased CDOM loads to mountain lakes might therefore not significantly affect their photic ratio. Sediment heat accumulation might nevertheless increase under a warmer climate, given constant water clarity. Consequences of climate change on the under-ice bottom DO dynamics in alpine lakes will then depend on which of the ice cover duration or the structure of the inverse stratification takes over.

Data Availability Statement

The sensors data that support the findings of this study are openly available in IS OLA (Observatory on LAkes) at https://si-ola.inrae.fr/si_lacs/login.jsf. Processed data are available at https://doi.org/10.5281/zenodo.7674243.

References

Bengtsson, L., and O. Ali-Maher. 2020. The dependence of the consumption of dissolved oxygen on lake morphology in ice covered lakes. Hydrol. Res. **51**: 381–391. doi:10.2166/nh.2020.150

Beutel, M. W. 2003. Hypolimnetic anoxia and sediment oxygen demand in California drinking water reservoirs. Lake Reserv. Manag. **19**: 208–221. doi:10.1080/07438140309354086

Birck, C., and others. 2013. Sentinel lakes: A network for the study and management of mountain lakes in the French Alps and in Corsica. Eco Mont J. Prot. Mt. Areas Res. **5**: 63–69. doi:10.1553/eco.mont-5-1s63

Bouffard, D., J. D. Ackerman, and L. Boegman. 2013. Factors affecting the development and dynamics of hypoxia in a large shallow stratified lake: Hourly to seasonal patterns. Water Resour. Res. **49**: 2380–2394. doi:10.1002/wrcr.20241

Brown, L. C., and C. R. Duguay. 2010. The response and role of ice cover in lake-climate interactions. Prog. Phys. Geogr. Earth Environ. **34**: 671–704. doi:10.1177/0309133310375653

Caldwell, T. J., and others. 2021. Drivers and projections of ice phenology in mountain lakes in the western United States. Limnol. Oceanogr. **66**: 995–1008. doi:10.1002/lno.11656

Carlson, B. Z., M. C. Corona, C. Dentant, R. Bonet, W. Thuiler, and P. Choler. 2017. Observed long-term greening of alpine vegetation—a case study in the French Alps. Environ. Res. Lett. **12**: 114006. doi:10.1088/1748-9326/aa84bd

Cavaliere, E., and others. 2021. The Lake ice continuum concept: Influence of winter conditions on energy and ecosystem dynamics. Journal of geophysical research. Biogeosciences **126**: e2020JG006165. doi:10.1029/2020JG006165

Couture, R.-M., H. A. de Wit, K. Tominaga, P. Kiuru, and I. Markelov. 2015. Oxygen dynamics in a boreal lake responds to long-term changes in climate, ice phenology, and DOC inputs. J. Geophys. Res. Biogeo. **120**: 2441–2456. doi:10.1002/2015JG003065

Cremona, F., A. Laas, P. C. Hanson, M. Sepp, P. Nõges, and T. Nõges. 2019. Drainage ratio as a strong predictor of allochthonous carbon budget in Hemiboreal Lakes. Ecosystems **22**: 805–817. doi:10.1007/s10021-018-0304-7

Davis, M. N., T. E. McMahon, K. A. Cutting, and M. E. Jaeger. 2020. Environmental and climatic factors affecting winter hypoxia in a freshwater lake: Evidence for a hypoxia refuge and for re-oxygenation prior to spring ice loss.

Hydrobiologia **847**: 3983–3997. doi:10.1007/s10750-020-04382-z

Devlin, S. P., M. J. Vander Zanden, and Y. Vadeboncoeur. 2016. Littoral-benthic primary production estimates: Sensitivity to simplifications with respect to periphyton productivity and basin morphometry. Limnol. Oceanogr.: Methods **14**: 138–149. doi:10.1002/lom3.10080

Fang, X., and H. G. Stefan. 1996. Dynamics of heat exchange between sediment and water in a lake. Water Resour. Res. **32**: 1719–1727. doi:10.1029/96WR00274

Flaim, G., D. Andreis, S. Piccolroaz, and U. Obertegger. 2020. Ice cover and extreme events determine dissolved oxygen in a Placid Mountain Lake. Water Resour. Res. **56**: e2020WR027321. doi:10.1029/2020WR027321

Fountain, A. G., J. L. Campbell, E. A. G. Schuur, S. E. Stammerjohn, M. W. Williams, and H. W. Ducklow. 2012. The disappearing cryosphere: Impacts and ecosystem responses to rapid cryosphere loss. BioScience **62**: 405-415. doi:10.1525/bio.2012.62.4.11

Gammons, C. H., and others. 2014. Stable isotopes track biogeochemical processes under seasonal ice cover in a shallow, productive lake. Biogeochemistry **120**: 359–379. doi:10.1007/s10533-014-0005-z

Ghane, A., and L. Boegman. 2023. The dissolved oxygen budget of a small Canadian shield lake during winter. Limnol. Oceanogr. **68**: 265–283. doi:10.1002/lno.12265

Gobiet, A., S. Kotlarski, M. Beniston, G. Heinrich, J. Rajczak, and M. Stoffel. 2014. 21st century climate change in the European Alps—a review. Sci. Total Environ. **493**: 1138–1151. doi:10.1016/j.scitotenv.2013.07.050

Golosov, S., and G. Kirillin. 2010. A parameterized model of heat storage by lake sediments. Environ. Model. Softw. **25**: 793–801. doi:10.1016/j.envsoft.2010.01.002

Golosov, S., O. A. Maher, E. Schipunova, A. Terzhevik, G. Zdorovennova, and G. Kirillin. 2007. Physical background of the development of oxygen depletion in ice-covered lakes. Oecologia **151**: 331–340. doi:10.1007/s00442-006-0543-8

Granados, I., M. Toro, S. Giralt, A. Camacho, and C. Montes. 2020. Water column changes under ice during different winters in a mid-latitude Mediterranean high mountain lake. Aquat. Sci. **82**: 30. doi:10.1007/s00027-020-0699-z

Hampton, S. E., and others. 2017. Ecology under lake ice. Ecol. Lett. **20**: 98–111. doi:10.1111/ele.12699

Heinz, G., J. Ilmberger, and M. Schimmele. 1990. Vertical mixing in Überlinger see, western part of Lake Constance. Aquat. Sci. **52**: 256–268. doi:10.1007/BF00877283

Hondzo, M., and G. Stefan. 1993. Lake water temperature simulation model. J. Hydraul. Eng. **119**: 1251–1273. doi:10.1061/(ASCE)0733-9429(1993)119:11(1251)

Jansen, J., and others. 2021. Winter limnology: How do hydrodynamics and biogeochemistry shape ecosystems under ice? Journal of geophysical research. Biogeosciences **126**: e2020JG006237. doi:10.1029/2020JG006237

Jassby, A., and T. Powell. 1975. Vertical patterns of eddy diffusion during stratification in castle Lake, California. Limnol. Oceanogr. **20**: 530–543. doi:10.4319/lo.1975.20.4.0530

Joint Research Centre, Institute for Environment Sustainability. 2012. *In* S. Poikane [ed.], Water framework directive intercalibration technical report. Part 2: Lakes. Publications Office. 10.2788/23415

Kincaid, D. W., E. C. Adair, D. Joung, J. D. Stockwell, and A. W. Schroth. 2022. Ice cover and thaw events influence nitrogen partitioning and concentration in two shallow eutrophic lakes. Biogeochemistry **157**: 15–29. doi:10.1007/s10533-021-00872-x

Kirillin, G., and others. 2012. Physics of seasonally ice-covered lakes: A review. Aquat. Sci. **74**: 659–682. doi:10.1007/s00027-012-0279-y

Larsen, S., T. Andersen, and D. O. Hessen. 2011. Predicting organic carbon in lakes from climate drivers and catchment properties. Global Biogeochem. Cycles **25**: GB3007. doi:10.1029/2010GB003908

Leppi, J. C., C. D. Arp, and M. S. Whitman. 2016. Predicting late winter dissolved oxygen levels in Arctic Lakes using morphology and landscape metrics. Environ. Manag. **57**: 463–473. doi:10.1007/s00267-015-0622-x

MacIntyre, S., A. Cortés, and S. Sadro. 2018. Sediment respiration drives circulation and production of CO_2 in ice-covered Alaskan arctic lakes. Limnol. Oceanogr. Lett. **3**: 302–310. doi:10.1002/lol2.10083

Magnuson, J. J., A. L. Beckel, K. Mills, and S. B. Brandt. 1985. Surviving winter hypoxia: Behavioral adaptations of fishes in a northern Wisconsin winterkill lake. Environ. Biol. Fishes **14**: 241–250. doi:10.1007/BF00002627

Magnuson, J. J., and others. 2000. Historical trends in lake and river ice cover in the northern hemisphere. Science **289**: 1743–1746. doi:10.1126/science.289.5485.1743

Malm, J., and others. 1998. Field study on currents in a shallow, ice-covered lake. Limnol. Oceanogr. **43**: 1669–1679. doi:10.4319/lo.1998.43.7.1669

Mathias, J. A., and J. Barica. 1980. Factors controlling oxygen depletion in ice-covered lakes. Can. J. Fish. Aquat. Sci. **37**: 185–194. doi:10.1139/f80-024

Mortimer, C. H., and F. J. H. Mackereth. 1958. Convection and its consequences in ice-covered lakes, p. 923–932. *In* SIL Proceedings, 1922–2010, Taylor and Francis online; **13**: 923–932. doi:10.1080/03680770.1956.11895490

Müller, B., L. D. Bryant, A. Matzinger, and A. Wüest. 2012. Hypolimnetic oxygen depletion in eutrophic lakes. Environ. Sci. Technol. **46**: 9964–9971. doi:10.1021/es301422r

Obertegger, U., B. Obrador, and G. Flaim. 2017. Dissolved oxygen dynamics under ice: Three winters of high-frequency data from Lake Tovel, Italy. Water Resour. Res. **53**: 7234–7246. doi:10.1002/2017WR020599

Olson, M. H., J. M. Fischer, C. E. Williamson, E. P. Overholt, and N. Theodore. 2017. Landscape-scale regulators of water transparency in mountain lakes: Implications of projected

glacial loss. Can. J. Fish. Aquat. Sci. **75**: 1169–1176. doi:10.1139/cjfas-2017-0215

Olson, M. H., J. M. Fischer, M. Hayashi, and C. E. Williamson. 2020. Meteorological drivers of interannual variation in transparency of mountain lakes. Arct. Antarct. Alp. Res. **52**: 424–434. doi:10.1080/15230430.2020.1800972

Parker, B. R., R. D. Vinebrooke, and D. W. Schindler. 2008. Recent climate extremes alter alpine lake ecosystems. Proc. Natl. Acad. Sci. USA **105**: 12927–12931. doi:10.1073/pnas.0806481105

Perga, M. E., R. Bruel, L. Rodriguez, Y. Guenand, and D. Bouffard. 2018. Storm impacts on alpine lakes: Antecedent weather conditions matter more than the event intensity. Glob. Chang. Biol. **24**: 5004–5016. doi:10.1111/gcb.14384

Preston, D. L., and others. 2016. Climate regulates alpine lake ice cover phenology and aquatic ecosystem structure. Geophys. Res. Lett. **43**: 5353–5360. doi:10.1002/2016GL069036

Råman Vinnå, L., I. Medhaug, M. Schmid, and D. Bouffard. 2021. The vulnerability of lakes to climate change along an altitudinal gradient. Commun. Earth Environ. **2**: 35. doi:10.1038/s43247-021-00106-w

Ramón, C. L., H. N. Ulloa, T. Doda, K. B. Winters, and D. Bouffard. 2021. Bathymetry and latitude modify lake warming under ice. Hydrol. Earth Syst. Sci. **25**: 1813–1825. doi:10.5194/hess-25-1813-2021

Salonen, K., M. Leppäranta, M. Viljanen, and R. D. Gulati. 2009. Perspectives in winter limnology: Closing the annual cycle of freezing lakes. Aquat. Ecol. **43**: 609–616. doi:10.1007/s10452-009-9278-z

Sharma, S., and others. 2021. Loss of ice cover, shifting phenology, and more extreme events in northern hemisphere lakes. J. Geophys. Res.: Biogeosci. **126**: e2021JG006348. doi:10.1029/2021JG006348

Smits, A. P., N. W. Gomez, J. Dozier, and S. Sadro. 2021. Winter climate and lake morphology control ice phenology and under-ice temperature and oxygen regimes in mountain lakes. J. Geophys. Res.: Biogeosci. **126**: e2021JG006277. doi:10.1029/2021JG006277

Song, S., and others. 2019. Under-ice metabolism in a shallow lake in a cold and arid climate. Freshw. Biol. **64**: 1710–1720. doi:10.1111/fwb.13363

Stefanovic, D. L., and H. G. Stefan. 2002. Two-dimensional temperature and dissolved oxygen dynamics in the littoral region of an ice-covered lake. Cold Reg. Sci. Technol. **34**: 159–178. doi:10.1016/S0165-232X(02)00003-4

Steinsberger, T., M. Schmid, A. Wüest, R. Schwefel, B. Wehrli, and B. Müller. 2017. Organic carbon mass accumulation rate regulates the flux of reduced substances from the sediments of deep lakes. Biogeosciences **14**: 3275–3285. doi:10.5194/bg-14-3275-2017

Stepanenko, V., I. Mammarella, A. Ojala, H. Miettinen, V. Lykosov, and T. Vesala. 2016. LAKE 2.0: A model for temperature, methane, carbon dioxide and oxygen dynamics in lakes. Geosci. Model Dev. **9**: 1977–2006. doi:10.5194/gmd-9-1977-2016

Terry, J. A., A. Sadeghian, and K.-E. Lindenschmidt. 2017. Modelling dissolved oxygen/sediment oxygen demand under ice in a shallow eutrophic prairie reservoir. Water **9**: 131. doi:10.3390/w9020131

Terzhevik, A., and others. 2009. Some features of the thermal and dissolved oxygen structure in boreal, shallow ice-covered Lake Vendyurskoe, Russia. Aquat. Ecol. **43**: 617–627. doi:10.1007/s10452-009-9288-x

Ulloa, H. N., K. B. Winters, A. Wüest, and D. Bouffard. 2019. Differential heating drives downslope flows that accelerate mixed-layer warming in ice-covered waters. Geophys. Res. Lett. **46**: 13872–13882. doi:10.1029/2019GL085258

Wang, X., and others. 2021. High-resolution mapping of ice cover changes in over 33,000 lakes across the north temperate zone. Geophys. Res. Lett. **48**: e2021GL095614. doi:10.1029/2021GL095614

Woolway, R. I., and C. J. Merchant. 2019. Worldwide alteration of lake mixing regimes in response to climate change. Nat. Geosci. **12**: 271–276. doi:10.1038/s41561-019-0322-x

Yang, B., and others. 2021. A new thermal categorization of ice-covered lakes. Geophys. Res. Lett. **48**: e2020GL091374. doi:10.1029/2020GL091374

Zdorovennova, G., and others. 2021. Dissolved oxygen in a shallow ice-covered lake in winter: Effect of changes in light, thermal and ice regimes. Water **13**: 2435. doi:10.3390/w13172435

Conflict of Interest

None declared.